Complex Langevin: Correctness criteria, boundary terms, and spectrum

Erhard Seiler,[1,*] Dénes Sexty,[2,†] and Ion-Olimpiu Stamatescu[3,‡]

[1]*Max-Planck-Institut für Physik (Werner-Heisenberg-Institut), Föhringer Ring 6, München, Germany*
[2]*Institute of Physics, NAWI Graz, University of Graz, Universitätsplatz 5, Graz, Austria*
[3]*Institut für Theoretische Physik, Universität Heidelberg, Heidelberg, Germany*

(Received 5 April 2023; accepted 28 November 2023; published 24 January 2024)

The Complex Langevin (CL) method to simulate "complex probabilities" ideally produces expectation values for the observables that converge to a limit equal to the expectation values obtained with the original complex "probability" measure. The situation may be spoiled in two ways: failure to converge and convergence to the wrong limit. It was found long ago that "wrong convergence" is caused by boundary terms; nonconvergence may arise from bad spectral properties of the various evolution operators related to the CL process. Here, we propose a class of criteria that allow one to rule out boundary terms and at the same time bad spectrum. Ruling out boundary terms in the equilibrium distribution arising from a CL simulation implies that the so-called convergence conditions are fulfilled. This in turn has been shown to guarantee that the expectation values of holomorphic observables are given by complex linear combinations of $\exp(-S)$ over various integration cycles. If the spectrum is pathological, however, the CL simulation in general does not reproduce the integral over the desired real cycle.

DOI: 10.1103/PhysRevD.109.014509

I. INTRODUCTION

The Complex Langevin (CL) stochastic process [1,2] describes the evolution of a probability distribution on the complexified configuration space, generated by the Fokker-Planck (FP) operator L^T. The probability distribution is supposed to converge to an equilibrium distribution, which reproduces the averages with respect to a complex measure of a class of holomorphic observables. In the last two decades, the Complex Langevin method enjoyed renewed interest, and it has been tested as a proposed solution to the sign problem in various systems such as the real time evolution of quantum field theories [3–9], various systems having nonzero chemical potential [10–13], and condensed matter systems [14,15]. The introduction of gauge cooling [16] made simulations possible also in gauge theories, allowing complex Langevin simulations in QCD to be carried out [17–23].

The application of the Complex Langevin equation is not without problems, though. Two possibilities of failure have been identified: The process may fail to converge, and it may converge to the wrong limit. Failure to converge may occur via exponentially increasing expectation values of certain observables, related to spectrum in the right half complex plane, or it may occur due to spreading of the probability measure, creating slowly decaying "skirts." In the latter case, expectation values of observables with high powers become mathematically undefined (thus failing to converge in practice).

The conservation of probability under the CL process guarantees a certain trivial stability: Expectation values of observables that are bounded on the complexified configuration space will remain bounded under the CL process. This shows that the semigroup generated by FP operator is bounded on an appropriate (Banach) space, and exponentially growing modes are not present for bounded observables. Unfortunately, this is irrelevant, as we need to consider holomorphic observables, which are not bounded unless they are constant. So, for the study of convergence and stability, a different mathematical setting is needed. This is done in the next section.

More serious is the problem of wrong convergence. This is typically due to the spreading out of the probability density, leading to slow decay (skirts) of the distribution and the occurrence of boundary terms, as discussed in [24,25]. This spreading can be tested by the control variables introduced in the next section. These are used to define a general class of criteria for correctness of the CL results; they are designed to rule out boundary terms, but they also rule out instability in the form of exponential or subexponential growth in the evolution of observables.

*ehs@mpp.mpg.de
†denes.sexty@uni-graz.at
‡I.O.Stamatescu@thphys.uni-heidelberg.de

The criteria are sufficient, provided certain additional conditions hold; so, they are not eliminating *all* possible failures of the CL method. These limitations as well as open problems are discussed in the last section.

We check some versions of the criteria numerically for a simple model of one variable in Sec. III and for a lattice model in Sec. IV. By direct numerical determination of the spectrum, it is revealed that violation of the criteria does not necessarily imply the presence of "bad" spectrum. There is a regime in which failure of the criteria indicate presence of boundary terms and "wrong convergence" of the CL simulations takes place, yet the direct determination of the spectrum shows absence of exponentially growing modes. In a simple model, we find that the appearance of unwanted spectrum is linked to the Lee-Yang zeroes; the significance of this fact is not yet entirely clear.

A word of caution is in order: The spectrum of a formally defined differential operator depends on the precise definition of the space on which it operates; likewise, the relation between the spectrum of an operator and the behavior of the semigroup it generates may be more subtle than we are used to from finite dimensions. Some of these points are addressed in the appendices.

There are, in principle, four possible combinations of boundary terms or no boundary terms, and bad spectrum or no bad spectrum (by bad spectrum, we mean eigenvalues of L_c, the complex Fokker-Planck operator, with positive real part), we find that, depending on the parameters chosen, bad spectrum and boundary terms may appear together, but boundary terms may also appear without bad spectrum, and, of course, there also is also a regime in which neither boundary terms nor bad spectrum occur. So, in the presence of boundary terms, there is always either wrong convergence or no convergence. Hence, the absence of boundary terms is a crucial condition for correctness; the absence of bad spectrum plays only a subsidiary role. Limitations of this statement, concerning situations where the absence of boundary terms, while necessary, is not sufficient for correctness, are discussed in Sec. V.

II. MATHEMATICAL GENERALITIES

To keep the notation simple, we carry out this discussion for one variable. The generalization to many variables requires some care, as discussed in Sec. IV.

A. Notation

We consider complex measures given by a complex density ρ which is holomorphic and given in terms of an action as

$$\rho(z) = \exp(-S(z)). \tag{1}$$

Expectation values of holomorphic observables observables $\mathcal{O}$ are given by integration over a suitable integration "cycle" (in the terminology of Witten [26]) γ:

$$\langle \mathcal{O}(z) \rangle = \frac{1}{Z} \int_\gamma \rho(z)\mathcal{O}(z)dz; \quad Z = \int_\gamma \rho(z)dz. \tag{2}$$

The CL equation is

$$dz(t) = K(z)dt + dw(t); \quad K(z) = \rho'(z)/\rho(z) = -S'(z);$$
$$K_x = \mathrm{Re}K, \qquad K_y = \mathrm{Im}K, \tag{3}$$

where dw is the increment of the Wiener process normalized as

$$\langle dw(t)^2 \rangle = 2dt. \tag{4}$$

The evolution of the probability density P on $\mathbb{C} = \mathbb{R}^2$ is given by The Fokker-Planck(FP) equation:

$$\partial_t P(x,y;t) = L^T P(x,y;t), \quad L^T = \partial_x^2 - \partial_x K_x - \partial_y K_y. \tag{5}$$

The evolution of observables is given by the transpose L of L^T

$$\partial_t \mathcal{O}(x,y;t) = L\mathcal{O}(x,y;t), \quad L = \partial_x^2 + K_x\partial_x + K_y\partial_y, \tag{6}$$

which simplifies for holomorphic observables to

$$\partial_t \mathcal{O}(z;t) = L_c\mathcal{O}(z;t), \qquad L_c = \partial_z^2 + K(z)\partial_z. \tag{7}$$

Formally, these linear evolutions are solved by exponential semigroups, such as $\exp(tL)$ etc.

B. A trivial fact

We start with a simple fact. Our probability measures on $\mathbb{C} \equiv \mathbb{R}^2$ are given by distributional "densities" $P(x,y;t)$ on $\mathbb{R}^2$, i.e., positive distributions (this includes δ distributions and $\mathcal{L}^1$ functions). We denote the standard (total variation) norm of measures on $\mathbb{R}^2$ by $\|.\|_1$. For a probability measure P, we have

$$\|P\|_1 = 1. \tag{8}$$

Since $\exp(tL^T)$ preserves probability, it is a contraction on the space of complex measures, i.e., for any complex density ρ and all $t \geq 0$,

$$\|\exp(tL^T)\rho\|_1 \leq \|\rho\|_1. \tag{9}$$

This means in particular that as an operator on $\mathcal{L}^1(\mathbb{R}^2)$, L^T has no unstable (exponentially growing) modes. More explicitly, this can be seen by noting that the

Fokker-Planck evolution operator $\exp(tL^T)$ has an integral kernel $\exp(tL^T)(x,y;x',y') \geq 0$ satisfying

$$\int dx'dy' \exp(tL^T)(x,y;x',y') = 1. \tag{10}$$

Mathematically, the natural space of observables would be the space of bounded continuous functions, a subspace of $\mathcal{L}^\infty$ in $\mathbb{C}$. On this space, $\exp(tL)$ is really the adjoint (transpose) of $\exp(tL^T)$ and

$$\int P(x,y;0)(\exp(tL)\mathcal{O})(x,y)dxdy \leq \|\mathcal{O}\|_\infty \equiv \sup_{x,y}|\mathcal{O}(x,y)|, \tag{11}$$

so the dual semigroup $\exp(tL)\mathcal{O}$ is again a contraction (i.e., has ∞ norm ≤ 1).

Unfortunately, $\mathcal{L}^\infty(\mathbb{R}^2)$ does not contain any nonconstant holomorphic functions, so clearly the space of observables has to be enlarged; that requires the space of allowed measures to be restricted in such a way that all observables in the enlarged space have well-defined expectation values.

C. Conditions on the space of probability measures

To get a nontrivial space of holomorphic observables, we have to consider weighted spaces of measures and observables. We define these spaces in terms of a strictly positive weight function $\sigma(x,y)$, growing at infinity, using the norms

$$\begin{aligned} \|f\|_{1,\sigma} &= \int \sigma(x,y)|f(x,y)|dxdy, \\ \|\mathcal{O}\|_{\infty,\sigma^{-1}} &= \sup_{x,y}|\mathcal{O}(x,y)/\sigma(x,y)|. \end{aligned} \tag{12}$$

By a slight abuse of notation, we denote the space of complex measures ρ on $\mathbb{C}$ with $\|\rho\|_{1,\sigma} < \infty$ by $\mathcal{L}^1_\sigma$ and the space of observables $\mathcal{O}$ with $\|\mathcal{O}\|_{\infty,\sigma^{-1}} < \infty$ by $\mathcal{L}^\infty_{1/\sigma}$. Of course, the space of observables also has to be chosen in such a way that the evolution operator L_c and the semigroup $\exp(tL_c)$ leave it invariant; this means that we cannot limit ourselves to a finite dimensional subspace, such as polynomials up to a given order.

The choice of the weight σ is dictated by the class of observables we want to consider: It has to be chosen such that they lie in $\mathcal{L}^\infty_{\sigma^{-1}}$. In other words, σ has to grow at least as fast as all the observables we want to consider. We should also choose σ so that it does not grow too much faster than the observables in our chosen space because we do not want it to cause a "false alarm" about slow decay.

For the noncompact case of $\mathbb{R}^d$, the usual set of observables consists of all polynomials, so we need σ to grow faster than any power at infinity. Possible choices are

$$\sigma_1(x,y) = \exp(\alpha(x^2+y^2)^{1/4}), \qquad \alpha > 0 \tag{13}$$

or

$$\sigma_2(x,y) = \exp(\alpha(\log(1+x^2+y^2))^2), \qquad \alpha > 0. \tag{14}$$

In the following, we use the second choice $\sigma \equiv \sigma_2$ with $\alpha = 1$.

For the case of a compact real configuration space, such as $U(1)$, the natural space of observables is spanned by the exponentials $\exp(inz)$, which grow exponentially in the imaginary direction. So, in this case, we need a stronger than exponential decay in the measure; we may choose, for instance,

$$\sigma_3(x,y) = \exp(|y|^\alpha), \quad \alpha > 1, \tag{15}$$

or

$$\sigma_4(x,y) = \exp(\alpha|y|\log(1+|y|)), \qquad \alpha > 0. \tag{16}$$

A similar growth of σ is needed for other compact groups like $SU(N)$ and hence for lattice gauge models.

It is not automatically true that $\exp(tL^T)$ is a contraction from $\mathcal{L}^1_\sigma$ to itself; we have to make an assumption quantifying the necessary decay of the measure evolving under the CL process:

Assumption A:

$$\|\exp(tL^T)P\|_{1,\sigma} \leq C\|P\|_{1,\sigma} \equiv C_\sigma \;\; \forall\, P \in \mathcal{L}^1_\sigma, \;\; t \geq 0, \tag{17}$$

with a constant C_σ independent of t. Written out, (17) says

$$\int P(x,y;t)\sigma(x,y)dxdy \leq C_\sigma. \tag{18}$$

The weight function plays the role of a *nonholomorphic* control variable, which is required to have a well-defined and bounded expectation value under the probability measure P evolving according to the Fokker-Planck equation.

If the CL process is ergodic, the choice of the initial distribution $P(x,y;0)$ does not matter, and we may, for instance, choose $P(x,y;0) = \delta(x)\delta(y)$, which is convenient for numerical checks.

Equations (17) or (18) imply

$$\left|\int P(x,y;t)\mathcal{O}(x,y)dxdy\right| \leq C_\sigma\|\mathcal{O}\|_{\infty,\sigma^{-1}}, \tag{19}$$

so expectation values of observables will be bounded in time; i.e., Assumption A implies that there are no exponentially growing modes showing up.

Assumption A is a criterion for correctness: Since it guarantees strong enough decay on $P(x,y;t)$, it implies the absence of boundary terms for the observables in $\mathcal{L}^\infty_{1/\sigma}$.

Condition A has the following relation to the "drift criterion" of [27]: The latter can be interpreted as a special case; it requires the existence of an $\alpha > 0$ such that Assumption A is satisfied for the choice $\sigma = \sigma_{d,\alpha}$ with

$$\sigma_{d,\alpha}(x,y) \equiv \exp(\alpha|K(x+iy)|). \tag{20}$$

This shows that for any polynomial S of higher than second degree, the drift criterion is stronger than the versions (13) and (14). In compact cases, the drift grows exponentially in the noncompact directions, so the control variable $\sigma_{d,\alpha}$ is again stronger than (15) and (16). It is in fact stronger than necessary; i.e., it might signal incorrectness of certain CL results when they are in fact correct. This has been found to actually occur in some cases of the one-link $U(1)$ model [28], but it might also happen for polynomial models.

Failure of Assumption A indicates insufficient deacy of the probability distribution, i.e., the presence of skirts. It should not be confused with "runaways," i.e., breakdown of the simulation after a finite time; this problem was eliminated in all cases encountered by the use of adaptive step size [29].

D. Implications for the spectrum

The Langevin operator L is the formal transpose of L^T. *It is the true transpose if and only if there are no boundary terms.* Since Assumption A guarantees the absence of boundary terms for observables in the appropriate space $\mathcal{L}^{\infty}_{1/\sigma}$, we have indeed

$$\int P(x,y;t)\mathcal{O}(x,y)dxdy = \int P(x,y;0)\mathcal{O}(x,y;t)dxdy, \tag{21}$$

where $\mathcal{O}(x,y;t) = (\exp(tL)\mathcal{O})(x,y)$ and $P(x,y;t) = (\exp(tL^T)P)(x,y)$.

Under Assumption A, the left-hand side of (21) is bounded uniformly in t, so the right-hand side is uniformly bounded as well; i.e., there are no unstable modes of L showing up.

In more detail, the argument goes as follows: By assumption,

$$\left|\int P(x,y;t)\mathcal{O}(x,y)dxdy\right| \le C\|P\|_{1,\sigma}\|\mathcal{O}(x,y)\|_{\infty,1/\sigma}; \tag{22}$$

choosing now

$$P(x,y;0) = \delta(x-x_0)\delta(y-y_0), \tag{23}$$

this bounds the left-hand side of (22) by

$$C\sigma(x_0,y_0)\|\mathcal{O}(x,y;0)\|_{\infty,1/\sigma}. \tag{24}$$

If there is no boundary term, i.e., (21) holds, we thus find

$$|\mathcal{O}(x_0,y_0;t)| \le C\sigma(x_0,y_0)\|\mathcal{O}(x,y;0)\|_{\infty,1/\sigma}, \tag{25}$$

which shows the absence of unlimited growth (exponentially or otherwise) in $\mathcal{O}(x+iy;t)$.

Restricting L to the subspace of holomorphic functions in $\mathcal{L}^{\infty}_{\sigma^{-1}}$, it can be replaced by L_c due to the Cauchy-Riemann equations, so under our assumption, L_c as well can have no unstable modes in this space.

III. QUARTIC MODEL

L. L. Salcedo [30] pointed out that a simple quartic model sheds light on some problems of the CL method. The model is defined by the action

$$S(x) = \frac{\lambda}{4}x^4 + \frac{m^2}{2}x^2 + hx, \tag{26}$$

which we investigate for $\lambda \ge 0$, $m^2 > 0$ and complex h (below we denote the imaginary part of h with h_I), corresponding to the complex density

$$\rho(x) \equiv \exp(-S(x)). \tag{27}$$

(Note that a lattice version of this model was studied in [31] using the Complex Langevin equation.) As remarked by Salcedo, given $\lambda > 0, m^2 \ge 0$, the partition function $Z(h) = \int \rho(x)dx$ vanishes for certain values purely imaginary of h (so-called Lee-Yang zeroes), leading to divergent expectation values of x^n, whereas the CL equation does not show anything special at these values; so, clearly the CL results cannot be correct. This fact is borne out by numerical studies, which show deviations between the exact results and the numbers produced by CL, becoming most dramatic near the Lee-Yang zeroes. Here, we want to point out that these deviations are linked to massive failures of Assumption A for Imh larger than some value h_c, so Eq. (25) does not hold there; we expect boundary terms to occur, and we cannot use the criterion to rule out spectrum of L_c in the right half plane. In the next subsection, the spectrum of L_c is directly determined numerically with the result that the appearance of unstable modes, while not coinciding with the appearance of boundary terms, is actually linked to the Lee-Yang zeroes (see also [31]).

To give a definite meaning to the spectrum of L_c, we consider it as an operator in the Hilbert space

$$\mathcal{H}_S = \mathcal{L}^2(\mathbb{R}, \exp(-\mathrm{Re}S)dx). \tag{28}$$

The spectrum is then the same as the spectrum of

$$-H = \exp(-S/2)L\exp(S/2) = \partial_x^2 + \frac{m^2}{2} + \frac{h^2}{4} + \left(\frac{3\lambda}{2} + \frac{m^4}{4}\right)x^2 - \frac{\lambda m^2}{2}x^4 - \frac{\lambda^2}{4}x^6 + \frac{hm^2}{2}x + \frac{\lambda h}{2}x^3, \tag{29}$$

considered as an operator on

$$\mathcal{H} = \mathcal{L}^2(\mathbb{R}, dx). \tag{30}$$

(Maybe it would be more natural to continue working in the Banach space defined in the previous section, but for spectral considerations, Hilbert spaces are more convenient.)

We are interested in complex "magnetic fields" h, so H is a Schrödinger operator with a complex potential.

Let us now consider purely imaginary h:

$$h = ih_I, \qquad h_I \in \mathbb{R}; \tag{31}$$

the spectrum of hermitian part $(H + H^\dagger)/2$ now reaches down to $-h_I^2/4 < 0$; in fact,

$$\psi_0^{(0)}(x) = \exp(-\mathrm{Re}S(x)/2) \tag{32}$$

is an eigenvector of $(H + H^\dagger)/2$ with eigenvalue $-h^2/4$. This shows that $\exp(tL_c)$ is *not* a contractive semigroup on $\mathcal{H}_S$. However, the numerics presented in the next subsection suggests that nevertheless

$$\|\exp(tL_c)\|_{\mathcal{H}_S} = \|\exp(-tH)\|_{\mathcal{H}} \tag{33}$$

remains bounded for all $t > 0$, provided h_I is small enough. $\psi_0 = \exp(-S(x)/2)$ is an eigenvector of $-H$ with eigenvalue 0, and presumably $\exp(tL_c)\phi$ converges to a multiple of ψ_0 for all $\phi \in \mathcal{H}_S$ in this case (see discussion in Appendix A.)

A. Checking Assumption *A*

We choose the weight function

$$\sigma_2(x, y) \equiv \exp[(\log(1 + x^2 + y^2))^2]; \tag{34}$$

this allows one to consider observables in the (Banach) space defined by the norm

$$\|\mathcal{O}(x + iy)\|_{\infty,1/\sigma} = \sup_{x,y}|\mathcal{O}(x + iy)|\exp[-(\log(1 + x^2 + y^2))^2], \tag{35}$$

which contains all polynomials in $z = x + iy$ and which also lie in the Hilbert space $\mathcal{H}_S$ (28). For comparison with the drift criterion, we also consider the weight functions $\sigma_{d,\alpha}(x, y)$ (20) with $\alpha_0 = 0.1$, $\alpha_1 = 0.5$, $\alpha_2 = 1.0$. Note that all functions $\sigma_{d,\alpha}$ grow like $\exp(\alpha|z|^3)$, much more strongly than σ.

In Fig. 1, we show the expectation values $\langle\sigma_2\rangle_t$ and $\langle\sigma_{d,\alpha}\rangle_t$ ($\alpha = 0.1, 0.5, 1.0$) under the CL process for short Langevin times t, for the parameters $\lambda = 1$, $m^2 = 0.1$, $h_I = 1.0$. We see a sharp increase of both quantities starting above $t = 1.2$; $\langle\sigma_{d,1.0}\rangle_t$ takes off a little earlier than the other expectation values. This is not surprising considering the stronger growth for $\alpha = 1.0$. So, for these parameters, Assumption *A* is violated with all choices of the weight function.

We also conclude from Fig. 1 that for the parameters chosen and $t < 1.2$, there are no visible boundary terms. This means that via integration by parts

$$\int P(x,y;t)\mathcal{O}(x+iy)dxdy = \int P(x,y;0)\mathcal{O}(x+iy;t)dxdy. \tag{36}$$

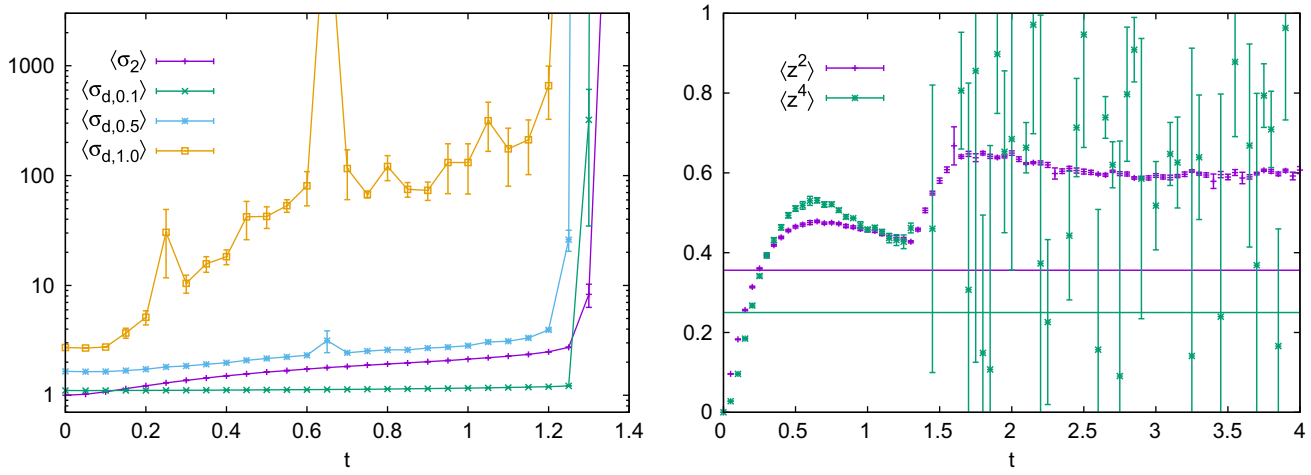

FIG. 1. $\langle\sigma_2\rangle_t$, $\langle\sigma_\alpha\rangle_t$, $\alpha = 0.1, 0.5, 1.0$ (left) and $\langle z^2\rangle_t$, $\langle z^4\rangle_t$ (right) vs Langevin time t, all averaged over 500,000 trajectories starting at the origin; parameters $\lambda = 1$, $m^2 = 0.1$, $h = 1.0i$. The horizontal lines give the "correct" equilibrium values.

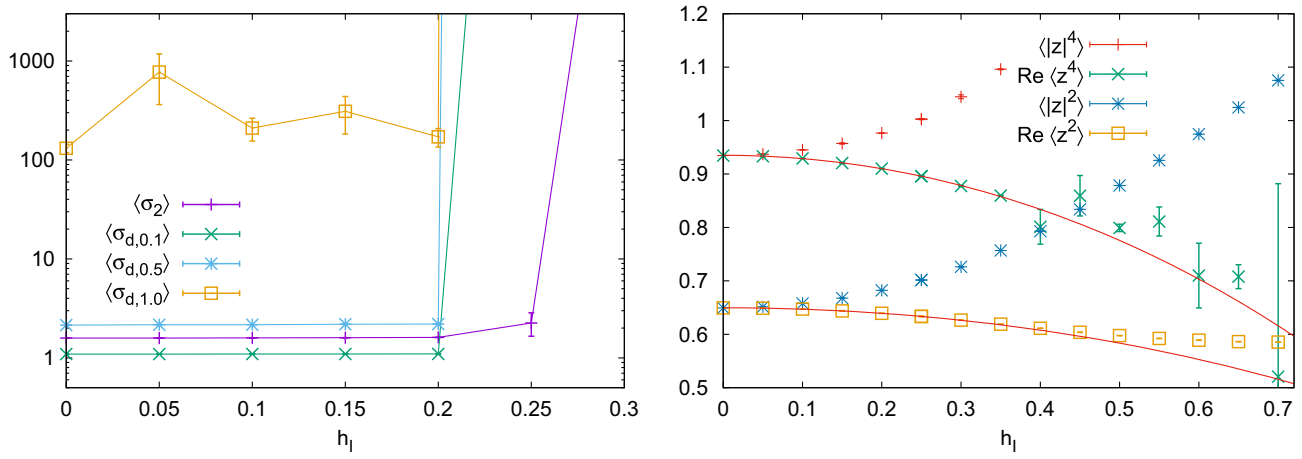

FIG. 2. Equilibrium CL results. Left: $\langle\sigma_2\rangle_t$ and $\langle\sigma_\alpha\rangle_t$, $\alpha = 0.1, 0.5, 1.0$ vs. $h_I = \mathrm{Im}h$, at $\mathrm{Re}h = 0$. Right: $\mathrm{Re}\langle z^2\rangle$ and $\mathrm{Re}\langle z^4\rangle$ as well as $\langle|z|^2\rangle$ and $\langle|z|^4\rangle$ vs. $h_I = \mathrm{Im}h$, at $\mathrm{Re}h = 0$; red lines: exact results.

Notice that increasing t up to 1.2, the data tend toward the correct equilibrium values, but before they can reach them, boundary terms appear and drive the results away from the correct ones (for $\langle z^2\rangle$) or make it impossible to determine them due to huge fluctuations (for $\langle z^4\rangle$). In other models [24,25], it was found that for suitable choice of parameters, there is a "plateau" in t, i.e., an interval in t in which the CL results were consistent with the correct ones, before the boundary terms appeared. For the model at hand, this situation also occurs for smaller values of h_I.

The distribution appears for $t < 1.2$ to decay faster than $1/\sigma_2$ and $1/\sigma_{d,\alpha}$; for larger t, the decay becomes slower, probably powerlike, leading to boundary terms and failure of CL.

It is possible to understand why around $t = 1.2$, the character of the CL process changes, and a skirt begins to show up: since we have no noise in the imaginary (y) direction, motion in this direction cannot be faster than that determined by the deterministic equation

$$\dot{y} = K_y, \qquad K_y(x,y) = -m^2 y - 3\lambda x^2 y + \lambda y^3 - h_I. \quad (37)$$

The flow pattern of the drift is such that $|K_y|$ has the largest downward size for $x = 0$; in fact, the solution of (37) will reach $-\infty$ after a finite time t_c. Since we are starting the process at the origin, for a time $t < t_c$, in the presence of noise in the x direction, no value lower than $y_0(t)$ can be reached, so $P(x, y; t)$ is supported in a strip $y_0(t) < y < 0$, and it is well localized in x, so no skirt can arise. t_c is determined from (37) by

$$t_c = \int_0^{-\infty} \frac{dy'}{K_y(0,y')}; \quad (38)$$

for $h_I = 1$, this gives

$$t_c = 1.25125. \quad (39)$$

In Fig. 2 (left panel), we present equilibrium values for $\lambda = 1$, $m^2 = 0.1$, varying h_I from 0 to 1. We show expectation values of σ_2, as well as $\sigma_{d,\alpha}$ ($\alpha = 0.1$, 0.5, 1.0); in the right panel, we show $\mathrm{Re}\langle z^2\rangle$ and $\mathrm{Re}\langle z^4\rangle$ as well as $\langle|z|^2\rangle$ and $\langle|z|^4\rangle$. We see that $\langle\sigma_2\rangle$ blows up at $h_I = 0.25$, while $\langle\sigma_{d,\alpha}\rangle$ blow up at already at $h_I = 0.2$; $\langle z^4\rangle$ starts deviating from the exact value around $h_I = 0.3$, whereas $\langle z^2\rangle$ starts showing already considerable deviation from the exact value starting at $h_I = 0.4$. At $h_I = 0.3$, the observable $\langle z^4\rangle$ starts to show increasing errors, while the control variables show huge values $\log(\langle\sigma_2\rangle) \simeq O(10 - 100)$.

We should remark it does not make sense to expect correctness for low powers and failure for the higher ones because that would mean failure of the "consistency conditions" linking different powers (see [32]). This again shows that it is necessary to work in a space of observables invariant under L_c and $\exp(tL_c)$.

We should also note that with our choice of purely imaginary h, the exact values of $\langle z^n\rangle$ for n even are purely real, whereas for n odd, they are purely imaginary. As for the CL values, due to the symmetry $x \to -x$ of the drift force K, this is also true as long as we have convergence.

We conclude from Fig. 2 that for $\lambda = 1$, $h_I \leq 0.25$ there are no visible boundary terms; the values of $\mathrm{Re}\langle z^n\rangle$ agree within the errors with the exact ones (the same is true for the imaginary parts), and L^T as well as L_c have no spectrum in the right-hand plane.

It should be noted that the first Lee Yang zero for our choice $\lambda = 1, m^2 = 0.1$ is at $h_1 \approx 2.52i$, so the blowup of $\langle\sigma\rangle$ both for finite t (Fig. 1) and for the equilibrium in Fig. 2 happens for $|h_I|$ much smaller than $|h_1|$. This is because the form of Assumption A we used is sufficient but not actually necessary to rule out "unstable modes." In the next subsection, it is shown by direct numerics that spectrum in the right half plane only appears for $|h_I| > |h_1|$.

It is also noteworthy that apparently it does not make much difference whether one chooses σ_2 or one of the $\sigma_{d,\alpha}$ as control variables as long as α is not too large: The blowup happens pretty much in the same place for the different α values, both in t and in h.

However, the simulations, together with the results of the next subsection, also make manifest that the spectrum in the left-hand plane alone does not guarantee correctness because it does not rule out boundary terms. The massive failure of expectation values $\langle z^2\rangle$ and $\langle z^4\rangle$ long before the first Lee-Yang zero shows this clearly. We also look at boundary terms for the observables z and z^2; as explained in [24,25]), they are obtained as

$$B_k(\mathcal{O}) = \lim_{C\to\infty}\int_{|z|^2\le C} P(x,y;t=\infty)L_c^k\mathcal{O}(z) \quad k=1,2,3,\ldots,$$
$$\mathcal{O}=z \quad \text{and} \quad z^2. \tag{40}$$

In Fig. 3, we show the plot of the boundary terms of these observables. As one observes, the first boundary term of z seems to be consistent with zero (in the infinite cutoff limit) for all magnetic fields; however, the second boundary term is nonzero above $h_I > 0.5$. For the observable z^2, already the first boundary term shows nonzero values above $h_I > 0.5$. This confirms the assessment made above using the control variables σ_2 and $\sigma_{d,\alpha}$.

B. Direct determination of the spectrum

In this section, we investigate the spectrum of the L_c operator for the model (26), given by

$$L_c = \partial_z^2 + K(z)\partial_z = \partial_z^2 - (m^2 z + \lambda z^3 + h)\partial_z. \tag{41}$$

For the numerical investigation, we used several bases $e_i^{(a)}$:

$$e_n^{(1)} = z^n, \qquad e_n^{(2)} = z^n e^{-z^2},$$
$$e_n^{(3)} = z^n e^{-S(z)/2}, \qquad e_n^{(4)} = \Phi_n(z), \tag{42}$$

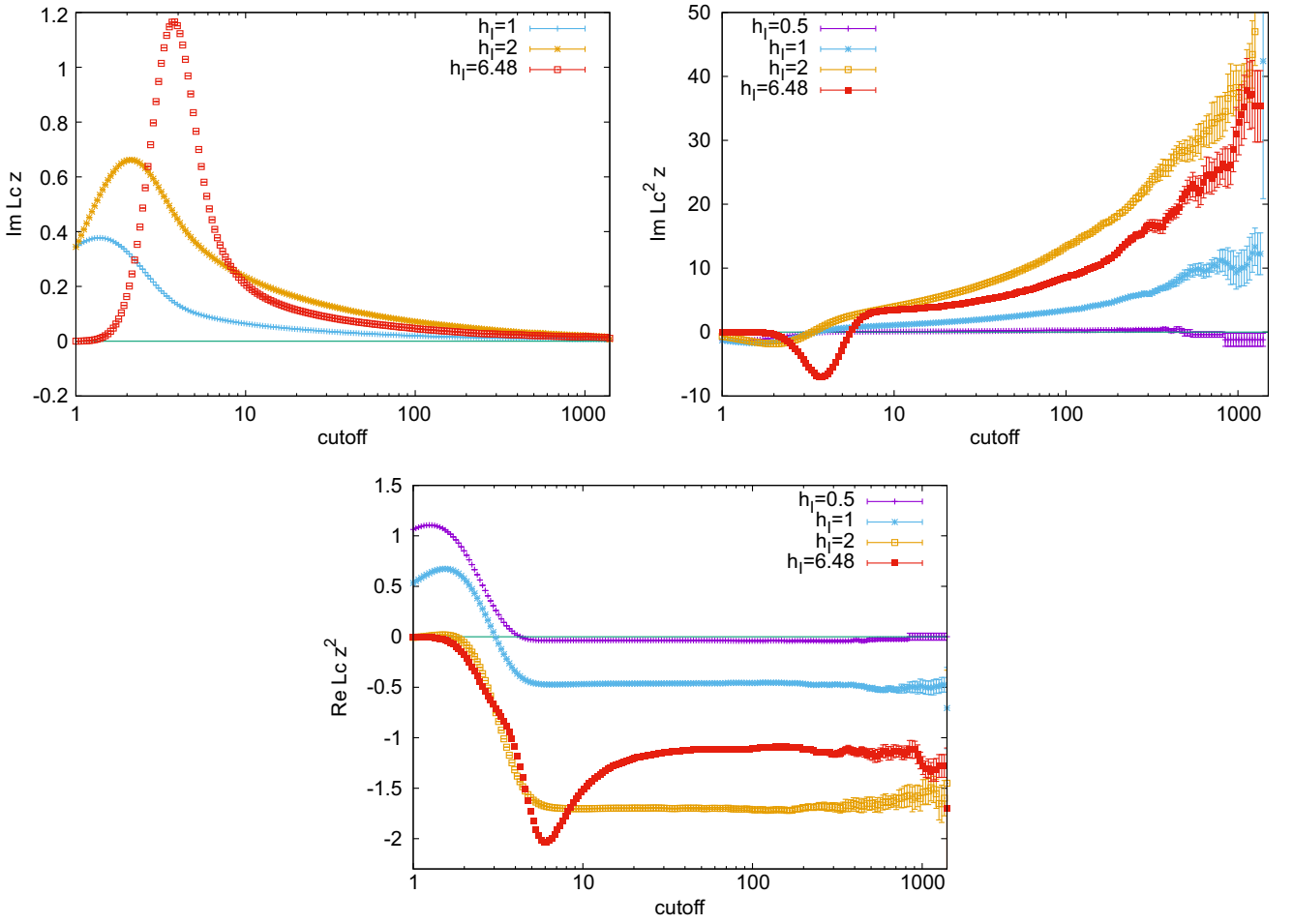

FIG. 3. The boundary terms in the quartic model (26) for $m^2 = 0.1$, $\lambda = 1$ and $\mathrm{Re}h = 0$: the imaginary parts of the first and second boundary terms of the observable z and the real part of the first boundary term of the observable z^2 is shown as a function of the cutoff $C = |z|^2$, for various $h_I = \mathrm{Im}h$ values, as indicated.

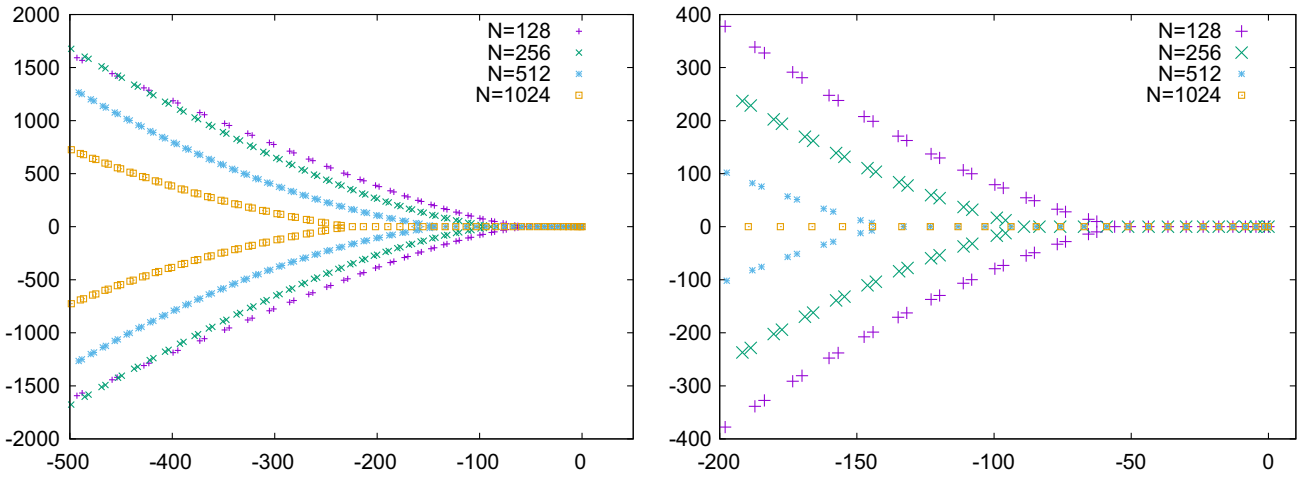

FIG. 4. The spectrum of the L_c operator at $\lambda = 1, m^2 = 0.1, h = 0$. On the right panel, a part of the spectrum closer to zero is shown.

where $e_n^{(1)}$ is the monomial basis, and $\Phi_n(z)$ are the eigenfunctions of the Hamiltonian of the corresponding harmonic oscillator. We truncate these bases using the first N basis vectors and calculate the spectrum of the resulting $N \times N$ (in general complex) matrix using the QR algorithm with explicit shifts [33]. The numerical diagonalization requires the usage of high precision numbers; e.g., at $N = 1024$, we use floating point numbers with a mantissa of 1024 bits to avoid the appearance of spurious eigenvalues due to precision loss.

To transform L_c into the bases given above, one writes, e.g.,

$$\mathcal{O}(z,t) = \sum \alpha_n(t) z^n e^{-Az^2}, \tag{43}$$

where $A = 0$ gives the monomial base $e^{(1)}$, and $A = 1$ gives the base $e^{(2)}$. One than calculates

$$\begin{aligned}(\partial_z + K(z))\partial_z \mathcal{O} = \sum_n \alpha_n [&n(n-1)z^{n-2} - 4Az^n n - 2Az^n \\ &+ 4A^2 z^{n+2} - m^2 n z^n - \lambda n z^{n+2} - h n z^{n-1} \\ &+ 2Am^2 z^{n+2} + 2A\lambda z^{n+4} + 2Ahz^{n+1}] e^{-Az^2}.\end{aligned} \tag{44}$$

Thus, L_c in this basis is given by

$$\begin{aligned}(L_c)_{nk} = &(n+2)(n+1)\delta_{n+2,k} - (4An + nm^2 + 2A)\delta_{n,k} \\ &+ (4A^2 - (n-2)\lambda + 2Am^2)\delta_{n-2,k} + 2A\lambda\delta_{n-4,k} \\ &+ 2Ah\delta_{n-1,k} + h(n+1)\delta_{n+1,k}.\end{aligned} \tag{45}$$

First we investigated the convergence of the spectrum as the truncation is improved. At $h = 0$, the spectrum of L_c is known to consist of nonpositive real eigenvalues. In Fig. 4, we show the spectrum of L_c for zero magnetic field for different truncations in the $e^{(2)}$ basis. We observe that nonreal eigenvalues appear for the truncated matrices; however, as the truncation is improved, more and more eigenvalues appear on the real axis, and the converged eigenvalues are all real (and nonpositive). In principle, the spectrum of the L_c operator in other bases should converge to the same eigenvalues, provided the bases are related by a bounded linear map with a bounded inverse (for more general basis changes, this may fail; see Appendix A). The convergence rate (with increasing truncation), however, may be basis dependent even then. From the bases mentioned above, $e^{(2)}$ shows by far the fastest convergence rate.

Next we investigate the number of positive real-part eigenvalues (which make the L_c evolution of some observables unstable) as a function of the magnetic field h. At zero real part of the magnetic field, as Imh is increased, eigenvalues appear with positive real parts. As observed in Fig. 5, the number of such eigenvalues increases by one precisely at the Lee-Yang zeroes of the theory. For higher magnetic field magnitudes, higher truncation of the L_c operator has to be used for convergence, as observed in Fig. 5.

In Fig. 6, we show the number of eigenvalues with positive real part as a function of the complex h parameter. Note that by the Lee-Yang theorem, which applies here [34,35], zeroes only occur for purely imaginary h.

IV. THE XY MODEL

In this section, we test the proposed control variables of the correctness criterion for the three dimensional XY model defined by the action

$$S = -\beta \sum_x \sum_{\nu=0}^{2} \cos(\phi_x - \phi_{x+\hat{\nu}} - i\mu\delta_{\nu,0}), \tag{46}$$

where x represents the space-time coordinate on a $2+1$ dimensional cubic lattice, $x + \hat{\nu}$ is the neighboring lattice

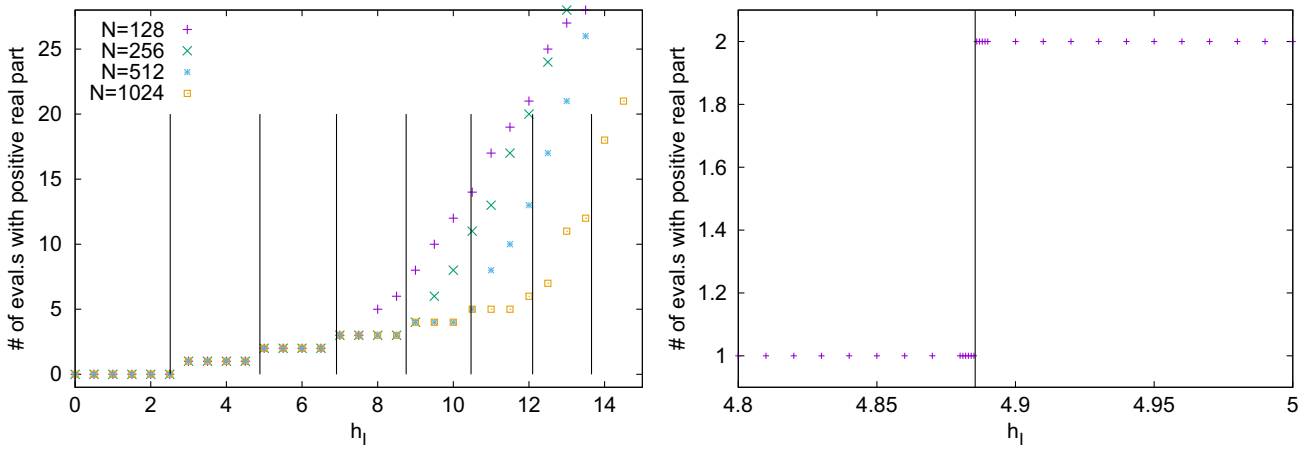

FIG. 5. The number of eigenvalues of L_c with positive real part as a function of the imaginary part of magnetic field h, at $\mathrm{Re}h = 0$, for different truncations in the basis $e^{(2)}$. The Lee-Yang zeroes of the theory are indicated by vertical lines. Right: zoom in around the second Lee-Yang zero. The parameters used are $\lambda = 1, m^2 = 0.1$.

point of x in the direction ν, and μ is the chemical potential. At $\mu > 0$, the action is in general complex, resulting in a sign problem hindering Monte Carlo simulations of the theory. This model has been previously investigated using the CLE in [36] and its boundary terms in [25]. The sign problem of this model can be solved using the worldline formulation [37]. To investigate the boundary terms in the XY model, we first defined the norm $N_{IM} = \max_x(\mathrm{Im}\phi_x)^2$, where the field configurations satisfying $N_{IM} < C$ for some real C enclose the real manifold in a bounded domain. We than investigate the observable

$$\theta(C - N_{IM})\frac{1}{N_s^2 N_t} L_c S[\phi_x] \tag{47}$$

as a function of the cutoff C. The limiting value for infinite cutoff gives the value of the boundary term [25]. In practice, the fluctuations of the observable increase for large C, so one reads of the value of the boundary term by, e.g., fitting a constant for large enough C values. In this case, we simply take the value at the cutoff $C = 8$, which is in the asymptotic region for all β values for the parameters considered here ($N_s = N_t = 8, \mu = 0.1$). It was observed in [36] that the CLE solution gives within errorbars correct values in the high β phase of the theory and incorrect results for small β. In Fig. 7, we show the boundary terms of the action density as a function of β, confirming this behavior.

We introduce the weight function

$$\sigma_{XY}(\mathrm{Re}\phi_x, \mathrm{Im}\phi_x) = \frac{1}{V}\sum_x \exp(\alpha|\mathrm{Im}\phi_x|^\gamma), \tag{48}$$

for the XY model, depending on all of the complexified ϕ variables on the lattice. As discussed in the previous sections, this weight function is then used to ascertain whether the probability distribution of the complexified process decays fast enough at infinity. Note that σ_{XY} has two parameters α and γ. The precise value of the γ

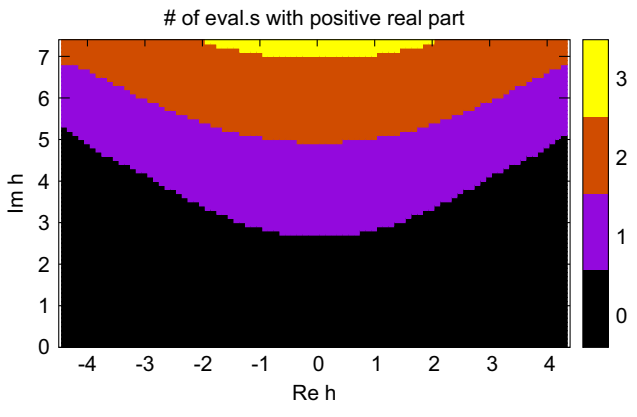

FIG. 6. The number of eigenvalues of L_c with positive real part on the complex plane of the magnetic field h, using the truncation $N = 512$, and the parameters $\lambda = 1, m^2 = 0.1$.

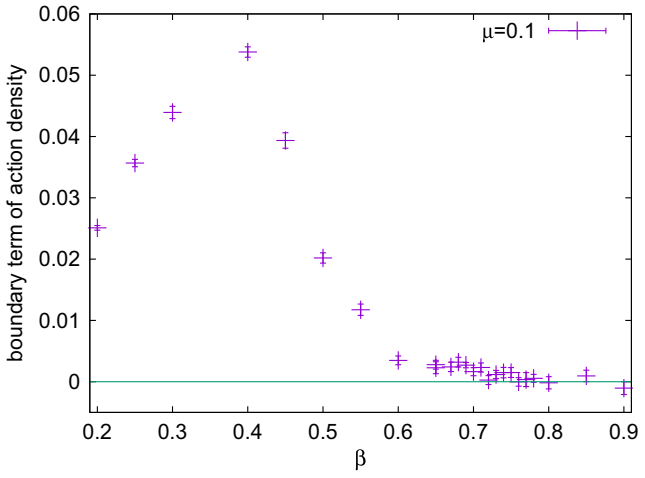

FIG. 7. The boundary terms of the action density in the XY model as a function of β.

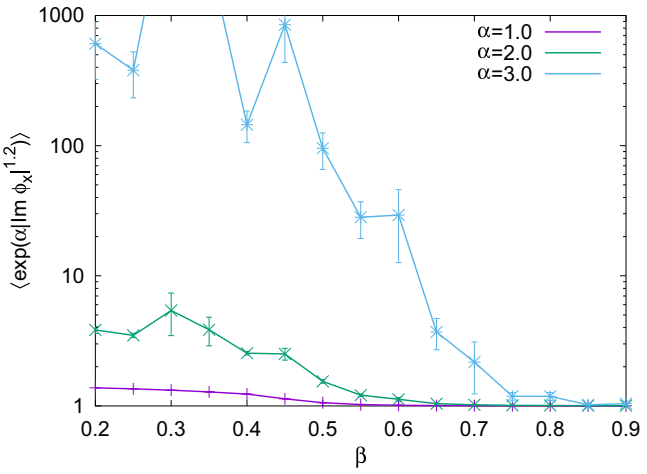

FIG. 8. The ensemble average of σ_{XY} defined in eq. (48) as a function of β, for various α values, at $\mu = 0.1$, measured on an 8^3 lattice. We used the exponent $\gamma = 1.2$ as indicated.

parameter is unimportant: As long as it is slightly above 1, the observable will be able to signal whether a faster than exponential decay in the probability distribution of ϕ_x is present. In Fig. 8, we show the ensemble average of σ_{XY} at various α values and at $\mu = 0.1$. One observes a behavior consistent with the boundary terms: At small β, large values and large fluctuations in the observable signal that the observable gets most of its contribution from the tails of the distribution, and thus, one should expect incorrect results. At large β, the values remain small, signaling fast decay and results consistent with the correct ones. Note that a certain experimentation with the parameter α is needed here: Using too small (large) α would mean that the observable is always small (large), but it seems there is a window of usable α's that correctly signal the behavior of the theory.

V. DISCUSSION AND OPEN PROBLEMS

A remaining question is if our Assumption A guarantees correctness of CL. What we showed here is that they imply that the spectrum of L_c and L_c^T lies in the left half of $\mathbb{C}$, and there are no boundary terms. However, this is not enough to guarantee correctness: Already in [38], it was pointed out that correctness is only guaranteed if also 0 is a *simple* (i.e., nondegenerate) eigenvalue of L_c^T.

What we can say is the following:

(i) Absence of boundary terms in the equilibrium measure of CL ensures that the "convergence conditions" (CC) [32] and the Schwinger-Dyson equations (SDE) are satisfied. This remains true also in the presence of a kernel.

(ii) As shown in [39], the SDE imply that the expectation values with the equilibrium measure are given by a complex linear combination of the integrations over inequivalent integration cycles. If there are several inequivalent integration cycles, each of them will represent a zero mode of L_c^T (here, we have to consider L_c^T as an operator acting on a space of linear functionals on the space of observables). Integration cycles connect different zeroes of $\rho(z) = \exp(-S(z)$, which may be finite or infinite, or they wind around compact directions of the configuration space. The real (physical) integration cycle is not always reproduced by CL, but the introduction of a kernel may remedy this.

(iii) In some cases, the existence of inequivalent integration cycles is also accompanied by nonergodicity of the CL process, i.e., the existence of different equilibrium distributions depending on the starting point. This will mean that the real Fokker-Planck operator L^T has more than one zero mode. However, there are also examples where the CL process is ergodic, yet the eigenvalue 0 of L_c^T is degenerate (see, for instance, the example in [39]).

Examples of the "mixing" of several integration cycles compromising the correctness of the CL simulations are plentiful; see, for instance, [39,40], as well as in Appendix B of [6], where for certain kernels, the spectrum of L_c is no longer on the left-hand side of the complex plane (which is signaled correctly by the criterion developed in this paper), the boundary terms seem to vanish, and in fact the results can be expressed as a complex linear combination of the integration cycles [39].

The special case of nonergodicity occurs in simple models with zeroes in the complex density ρ in [40]. If ρ has a finite zero on the original real integration cycle, there are typically at least two inequivalent integration cycles, starting at that zero and going to infinity in different directions. More zeroes lead to supplementary cycles connecting two zeroes. Such cycles also occur in the case of compact models, connecting two finite zeroes. In fact, here, it is easy to see that the eigenvalue 0 of L_c^T is degenerate: We may multiply $\psi_0 = \exp(-S)$ by the characteristic function of an interval between two zeroes (one of which may be at infinity), thereby producing a new eigenfunction of L_c^T with eigenvalue 0.

However, ergodicity may also fail in simple quartic models without finite zeroes, for instance, for

$$S = \frac{\lambda}{4}(z^2 - (a+ib)^2)^2, \quad \lambda = 2., a = 3., b = 1., \quad (49)$$

where numerics strongly suggests that there are two different equilibrium distributions [28]. Another example of apparent nonergodicity is found in Appendix B of [6], in that case, involving CL with a constant kernel.

In a nonergodic situation, in particular, in the presence of zeroes of ρ, it may depend on the starting point of CL which integration cycle or which linear combination of cycles is represented. For lattice models, it is of course quite difficult to determine all the possible integration

cycles as well as the linear combination of them representing the original problem.

To summarize, we have located the main problems of the Complex Langevin method: first, insufficient decay of the probability distribution generated by the process, which leads to boundary terms and spoils the averages. Second, degeneracy of the zero mode of L_c^T, which is related to inequivalent integration cycles of the theory (this includes ergodicity problems). The first problem has been thoroughly studied both in simple models and in lattice simulations of realistic models. It can be tested for using an online measurement; sometimes even correction of the CL results can be performed [24,25]. In this paper, we have proposed some diagnostic observables that signal the first as well as the second problem.

These problems (especially the second one) need further investigation, probably with the introduction of (field-dependent) kernels. If a kernel has the effect of forcing the equilibrium distribution to stay close to the real, respectively, unitary (physical) manifold, this could alleviate the aforementioned problems, and the results will typically be correct [6–9].

ACKNOWLEDGMENTS

D. S. acknowledges the support of the Austrian Science Fund (FWF) through the Stand alone Project No. P36875. The numerical simulations for this project were carried out on GSC, the computing cluster of the University of Graz.

APPENDIX A: SOME SUBTLE POINTS CONCERNING THE SPECTRUM OF NON-SELF-ADJOINT OPERATORS

Since in the 1980's the CL pioneers Klauder and Petersen [41] lamented about the … *conspicuous absence of general spectral theorems …,* there has been a lot of research on this issue; several textbooks have appeared, which deal with the thorny question of the spectrum of unbounded operators that are not normal operators on a Hilbert space; see, e.g., [42–44]. There are, however, still many open problems. We want to mention a few unpleasant facts showing that the situation is much more subtle than in the case of normal operators or finite matrices.

(1) The spectrum is not always invariant under similarity transformations. A simple example is found in [44], Example 9.3.200: Consider

$$L = \partial_x^2 + b\partial_x \quad \text{on } \mathcal{L}^2(\mathbb{R}). \tag{A1}$$

By a similarity transformation well-known from CL, L is transformed into $-H$

$$-H = \exp(bx/2) L \exp(-bx/2) = \partial_x^2 + \frac{b^2}{4}. \tag{A2}$$

The spectra are easily seen, using Fourier transformation, to be

$$\begin{aligned} \mathrm{spec}(L) &= \{\lambda \in \mathbb{C} | \lambda = -p^2 + ibp, p \in \mathbb{R}\} \\ \mathrm{spec}(-H) &= \{\lambda \in \mathbb{R} | \lambda = -p^2 - b^2/4, p \in \mathbb{R}\}, \end{aligned} \tag{A3}$$

i.e., a parabola vs a half line.

(2) The fact that the spectrum of L is in the left half plane does not preclude growth of the semigroup $\exp(tL)$, even in the finite dimensional case.

The simplest example is given by $L = a^\dagger$, where $a^\dagger$ is the creation operator of one fermion mode. The semigroup is $\exp(ta^\dagger) = 1 + ta^\dagger$, which shows linear growth, even though

$$\mathrm{spec}(a^\dagger) = \{0\}, \qquad \mathrm{spec}(\exp(ta^\dagger)) = \{1\}. \tag{A4}$$

There are examples of much stronger subexponential growth, given by Volterrra operators, whose spectrum consists again just of the origin.

However, even exponential growth can happen for an operator whose spectrum lies entirely in the closed left half plane; see [44], Theorem 8.2.9, which discusses an infinite matrix example due to Zabczyk.

(3) It is not true in all generality that the spectrum of $\exp(tL)$ is given by the exponential of the spectrum of L. This requires that the so-called spectral mapping principle holds. A detailed discussion is given in [42], Ch. 2.

(4) A useful condition is the following:

A closed operator L is called *dissipative*, if

$$\mathrm{Re}(\psi, L\psi) < 0 \tag{A5}$$

for all ψ in the domain of definition of L. There is a theorem, due to Lumer and Phillips [43], Cor. 3.17, showing that L defines a contractive semigroup; i.e., $\| \exp(tL) \| < 1 \ \forall \ t > 0$, if L is dissipative. The converse is also true; i.e., if L does not satisfy (A5), $\exp(tL)$ will not be contractive.

(5) Considering our Assumption A, it seems a natural setting would be in the context of Banach, rather than Hilbert spaces. In fact, the book by van Neerven is written that way.

APPENDIX B: EXAMPLE OF NONUNIQUE L_c EVOLUTION

The *real* one-pole model in the simplest case is defined by

$$\rho(x) = x^2 \exp(-\beta x^2). \tag{B1}$$

The kernel of $\exp(tL_c)$ is given in [45] as

$$\exp(tL_c)(x,y) = 2\frac{y}{x}\exp\left(\frac{\beta}{2}(x^2-y^2)\right)\exp(2\beta t)\sqrt{\frac{\beta}{\pi(1-e^{-4\beta t})}} \times \exp\left[-\frac{\beta(x^2+y^2)}{2\tanh(2\beta t)}\right]\exp\left(\frac{\beta xy}{\exp(2\beta t)}\right). \quad \text{(B2)}$$

It is easy to see that this has the unstable eigenmode $1/y$ with eigenvalue 2β for L_c, as found in [45]. The initial value problem

$$\partial_t \mathcal{O}(z;t) = L_c \mathcal{O}(z;t) \quad \text{with} \quad \mathcal{O}(z;0) = \frac{1}{z} \quad \text{(B3)}$$

thus has the solution

$$\mathcal{O}(z;t) = \exp(2\beta t)\frac{1}{z}. \quad \text{(B4)}$$

This solution is valid for $z \in \mathbb{C}\backslash\{0\}$ and is jointly analytic in t, z. As found in [45], the unstable mode is signaled also by a boundary term.

However, as remarked in the appendix of [45], this solution is not unique, even in the limit $\beta \to 0$. A second solution for $\beta = 0$ is

$$\mathcal{O}_{-1}(z;t) = \frac{1}{z}\mathrm{Erf}\left(\frac{z}{2\sqrt{t}}\right); \quad \text{(B5)}$$

for nonzero β, it is

$$\mathcal{O}_{-1}(z;t) = \frac{1}{z}\exp(2\beta t)\mathrm{Erf}(c(\beta,t)z), \quad \text{(B6)}$$

with

$$c(\beta,t) = \sqrt{\frac{\beta\exp(-4\beta t)}{1-\exp(-4\beta t)}}. \quad \text{(B7)}$$

This solution is for $t > 0$ holomorphic in $z \in \mathbb{C}$, but it has an essential singularity at $t = 0$. On closer inspection, it is seen that as soon as $|\mathrm{Im}z| > |\mathrm{Re}z|$, the solution blows up as $t \to 0$, so it does not solve the initial value problem everywhere. It solves it only in the wedge $|\mathrm{Im}z| < |\mathrm{Re}z|$.

The solution (B5) is correctly represented by the real Langevin process on the positive or negative real half-axis. There is no boundary term and no unstable mode.

If we want to simulate the one-pole model on a line parallel to the real axis, only the first solution can be used. The CL process then produces a superposition of the positive and negative half-lines (the coefficients actually depend on the starting point of the process), as shown in [39]; the CL process is not ergodic. There is an unstable mode present, CL produces an incorrect result, and there is a boundary term at the origin term signaling incorrectness [45].

[1] G. Parisi, On complex probabilities, Phys. Lett. **131B**, 393 (1983).
[2] J. R. Klauder, Stochastic quantization, Acta Phys. Aust. Suppl. **25**, 251 (1983).
[3] J. Berges and I. O. Stamatescu, Simulating nonequilibrium quantum fields with stochastic quantization techniques, Phys. Rev. Lett. **95**, 202003 (2005).
[4] J. Berges, S. Borsanyi, D. Sexty, and I. O. Stamatescu, Lattice simulations of real-time quantum fields, Phys. Rev. D **75**, 045007 (2007).
[5] J. Berges and D. Sexty, Real-time gauge theory simulations from stochastic quantization with optimized updating, Nucl. Phys. **B799**, 306 (2008).
[6] D. Alvestad, R. Larsen, and A. Rothkopf, toward learning optimized kernels for Complex Langevin, J. High Energy Phys. 04 (2023) 057.
[7] K. Boguslavski, P. Hotzy, and D. I. Müller, Stabilizing Complex Langevin for real-time gauge theories with an anisotropic kernel, arXiv:2212.08602.
[8] N. M. Lampl and D. Sexty, Real time evolution of scalar fields with kernelled Complex Langevin equation, arXiv:2309.06103.
[9] D. Alvestad, A. Rothkopf, and D. Sexty, Lattice real-time simulations with learned optimal kernels, arXiv:2310.08053.
[10] G. Aarts, Can stochastic quantization evade the sign problem? The relativistic Bose gas at finite chemical potential, Phys. Rev. Lett. **102**, 131601 (2009).
[11] G. Aarts and F. A. James, Complex Langevin dynamics in the SU(3) spin model at nonzero chemical potential revisited, J. High Energy Phys. 01 (2012) 118.
[12] A. Mollgaard and K. Splittorff, Full simulation of chiral random matrix theory at nonzero chemical potential by Complex Langevin, Phys. Rev. D **91**, 036007 (2015).
[13] J. Bloch, J. Glesaaen, J. J. M. Verbaarschot, and S. Zafeiropoulos, Complex Langevin simulation of a random matrix model at nonzero chemical potential, J. High Energy Phys. 03 (2018) 015.

[14] T. Hayata and A. Yamamoto, Complex Langevin simulation of quantum vortices in a Bose-Einstein condensate, Phys. Rev. A **92**, 043628 (2015).
[15] C. E. Berger, L. Rammelmüller, A. C. Loheac, F. Ehmann, J. Braun, and J. E. Drut, Complex Langevin and other approaches to the sign problem in quantum many-body physics, Phys. Rep. **892**, 1 (2021).
[16] E. Seiler, D. Sexty, and I. O. Stamatescu, Gauge cooling in Complex Langevin for QCD with heavy quarks, Phys. Lett. B **723**, 213 (2013).
[17] D. Sexty, Simulating full QCD at nonzero density using the Complex Langevin equation, Phys. Lett. B **729**, 108 (2014).
[18] K. Nagata, J. Nishimura, and S. Shimasaki, Complex Langevin calculations in finite density QCD at large μ/T with the deformation technique, Phys. Rev. D **98**, 114513 (2018).
[19] J. B. Kogut and D. K. Sinclair, Applying complex langevin simulations to lattice QCD at finite density, Phys. Rev. D **100**, 054512 (2019).
[20] D. Sexty, Calculating the equation of state of dense quark-gluon plasma using the Complex Langevin equation, Phys. Rev. D **100**, 074503 (2019).
[21] M. Scherzer, D. Sexty, and I. O. Stamatescu, Deconfinement transition line with the Complex Langevin equation up to $\mu/T \sim 5$, Phys. Rev. D **102**, 014515 (2020).
[22] Y. Ito, H. Matsufuru, Y. Namekawa, J. Nishimura, S. Shimasaki, A. Tsuchiya, and S. Tsutsui, Complex Langevin calculations in QCD at finite density, J. High Energy Phys. 10 (2020) 144.
[23] F. Attanasio, B. Jäger, and F. P. G. Ziegler, QCD equation of state via the Complex Langevin method, arXiv:2203.13144.
[24] M. Scherzer, E. Seiler, D. Sexty, and I. O. Stamatescu, Complex Langevin and boundary terms, Phys. Rev. D **99**, 014512 (2019).
[25] M. Scherzer, E. Seiler, D. Sexty, and I. O. Stamatescu, Controlling Complex Langevin simulations of lattice models by boundary term analysis, Phys. Rev. D **101**, 014501 (2020).
[26] E. Witten, Analytic continuation of Chern-Simons theory, AMS/IP Stud. Adv. Math. **50**, 347 (2011), arXiv:1001.2933.
[27] K. Nagata, J. Nishimura, and S. Shimasaki, Argument for justification of the Complex Langevin method and the condition for correct convergence, Phys. Rev. D **94**, 114515 (2016).
[28] E. Seiler (unpublished).
[29] G. Aarts, F. A. James, E. Seiler, and I. O. Stamatescu, Adaptive stepsize and instabilities in Complex Langevin dynamics, Phys. Lett. B **687**, 154 (2010).
[30] L. L. Salcedo (private communication).
[31] F. Attanasio, M. Bauer, L. Kades, and J. M. Pawlowski, Searching for Yang-Lee zeros in O(N) models, Proc. Sci. LATTICE2021 (**2022**) 223.
[32] G. Aarts, F. A. James, E. Seiler, and I. O. Stamatescu, Complex Langevin: Etiology and diagnostics of its main problem, Eur. Phys. J. C **71**, 1756 (2011).
[33] G. H. Golub and C. F. Van Loan, *Matrix Computations* (JHU Press, Baltimore, Maryland, 2013).
[34] T. D. Lee and C. N. Yang, Statistical theory of equations of state and phase transitions. I. Theory of condensation, Phys. Rev. **87**, 404 (1952); II. Lattice gas and Ising model, Phys. Rev. **87**, 410 (1952).
[35] B. Simon and R. B. Griffiths, The $(\phi^4)_2$ field theory as a classical Ising model, Commun. Math. Phys. **33**, 145 (1973).
[36] G. Aarts and F. A. James, On the convergence of Complex Langevin dynamics: The Three-dimensional XY model at finite chemical potential, J. High Energy Phys. 08 (2010) 020.
[37] D. Banerjee and S. Chandrasekharan, Finite size effects in the presence of a chemical potential: A study in the classical non-linear O(2) sigma-model, Phys. Rev. D **81**, 125007 (2010).
[38] G. Aarts, E. Seiler, and I.-O. Stamatescu, The Complex Langevin method: When can it be trusted?, Phys. Rev. D **81**, 054508 (2010).
[39] L. L. Salcedo and E. Seiler, Schwinger–Dyson equations and line integrals, J. Phys. A **52**, 035201 (2019).
[40] G. Aarts, E. Seiler, D. Sexty, and I. O. Stamatescu, Complex Langevin dynamics and zeroes of the fermion determinant J. High Energy Phys. 05 (2017) 044; 01 (2018) 128(E).
[41] J. Klauder and W. P. Petersen, Spectrum of certain non-self-adjoint operators and solutions of Langevin equations with complex drift, J. Stat. Phys. **39**, 53 (1985).
[42] J. Van Neerven, *The Asymptotic Behavior of Semigroups of Linear Operators* (Birkhäuser-Verlag, Basel etc. 1996).
[43] K.-J. Engel and R. Nagel, *One-Parameter Semigroups for Linear Evolution Equations* (Springer-Verlag, Berlin etc. 2000).
[44] E. B. Davies, *Linear Operators and Their Spectra* (Cambridge University Press, Cambridge, England, 2007).
[45] E. Seiler, Complex Langevin: Boundary terms at poles, Phys. Rev. D **102**, 094507 (2020).